

## Probing magnetic anisotropy effects in epitaxial CrO<sub>2</sub> thin films

L. Spinu,<sup>1</sup> H. Srikanth,<sup>1</sup> A. Gupta,<sup>2</sup> X. W. Li,<sup>3</sup> and Gang Xiao<sup>3,4</sup>

<sup>1</sup>Advanced Materials Research Institute, University of New Orleans, New Orleans, Louisiana 70148

<sup>2</sup>IBM T. J. Watson Research Center, Yorktown Heights, New York 10598

<sup>3</sup>Physics Department, Brown University, Providence, Rhode Island 02912

<sup>4</sup>Department of Physics, Hong Kong University of Science & Technology, Kowloon, Hong Kong

(Received 19 June 2000)

The magnetic anisotropy in ferromagnetic chromium dioxide thin films ( $T_c \sim 393$  K) grown epitaxially on (100) TiO<sub>2</sub> substrates, is probed using precise rf transverse susceptibility ( $\chi_T$ ) measurements. Singular peaks in  $\chi_T$  are observed that are associated with the anisotropy ( $\pm H_K$ ) and switching ( $\pm H_s$ ) fields in CrO<sub>2</sub>. Theoretical calculations of  $\chi_T$  based on a simple coherent rotation model display remarkable agreement with the experimental data, indicating that these thin films behave like single-domain magnetic particles. Magneto-elastic contributions to the total anisotropy energy are needed to describe the evolution of  $\chi_T$  peaks at lower temperatures.

Magnetoelectronics is a field of current topical interest and several materials exhibiting a high degree of spin polarization are being investigated for use in tunnel junctions and spin-based devices.<sup>1,2</sup> Among the different classes of materials, chromium dioxide (CrO<sub>2</sub>) ranks as the leading contender for exhibiting complete spin polarization at the Fermi level and is classified as being *half-metallic*.<sup>3</sup> Band-structure calculations predict almost 100% spin polarization for this system, and some experimental observations like spin-polarized photoemission<sup>4</sup> and superconducting point-contact spectroscopy<sup>5</sup> have validated this prediction. This property makes CrO<sub>2</sub> a very attractive candidate for the fabrication of magnetic tunnel junctions with enhanced low-field magnetoresistance. Large magnetoresistance has also been observed in granular powder compacts of chromium dioxide, where the effect is due to intergranular tunneling of spin polarized electrons.<sup>6</sup>

Structural, transport, and magnetic properties of chromium dioxide have been investigated by several groups.<sup>6–10</sup> As there is a thrust toward device miniaturization and achieving faster switching times, it is likely that magnetic recording materials will be operating at higher frequencies. In view of this, it is vital to obtain a good understanding of the dynamic magnetic response in CrO<sub>2</sub> for applied rf electromagnetic fields.

In this paper, we present rf transverse susceptibility ( $\chi_T$ ) measurements on high-quality epitaxially grown thin films of CrO<sub>2</sub>. Singular peaks are observed in  $\chi_T$  at the characteristic anisotropy fields that differ by an order of magnitude for static magnetic field ( $H$ ) applied parallel and perpendicular to the magnetic easy axis. We also observe evidence of the temperature dependent influence of strain in the films due to lattice mismatch between the film and substrate materials. All the observed data are well described by the Stoner–Wohlfarth coherent rotation model.<sup>11</sup>

CrO<sub>2</sub> is a metastable phase, and it is a challenge to obtain this phase using conventional thin film growth techniques under ambient conditions. The films used in this study were  $5 \times 5$  mm<sup>2</sup> in size and typically 2000 Å thick, grown on single-crystal (100) TiO<sub>2</sub> substrates using chemical vapor

deposition technique at atmospheric pressure.<sup>12</sup> Both CrO<sub>2</sub> and TiO<sub>2</sub> have rutile structures, but the lattice mismatch between the film and substrate has been noted to be significant, leading to an anisotropic in-plane tensile strain being imposed on the film.

The structural and magnetic properties of these films have been extensively characterized using x-ray diffraction and superconducting quantum interference device (SQUID) magnetometry.<sup>8,9,12</sup> The films used in this study showed a ferromagnetic Curie temperature of 393 K, with well-defined magnetic easy and hard axis along the [001] ( $c$  axis) and [010] ( $b$  axis), respectively. The  $M$ - $H$  data measured at room and low temperatures with a SQUID magnetometer are shown in Figs. 1(a) and 1(b) with magnetic fields applied parallel and perpendicular to the easy axis. An important property of CrO<sub>2</sub> is the very large in-plane uniaxial anisotropy that is reflected in the shapes of the hysteresis loops as seen in Fig. 1. As we show in this paper, this anisotropy can be probed sensitively, and explored in great detail using precise transverse susceptibility experiments.

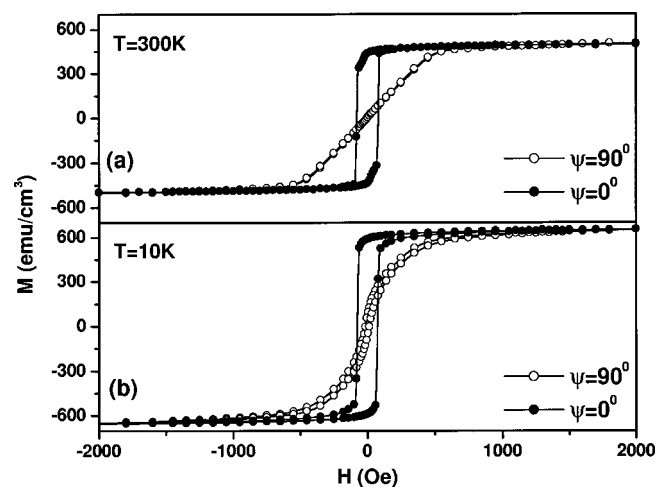


FIG. 1.  $M$ - $H$  data measured with a SQUID magnetometer with applied fields parallel and perpendicular to the easy axis for (a) 300 K and (b) 10 K.

Transverse susceptibility is an extremely useful method to study the magnetic properties of materials in general and the effective anisotropy in particular.<sup>13–16</sup> The basic idea behind these experiments is to measure the change in transverse component of the magnetization as the applied static field is varied. Recently, we developed a way to conduct transverse susceptibility measurements at radio frequencies with high sensitivity,<sup>17</sup> and used this method to explore the anisotropy in magnetic nanoparticles.<sup>18</sup>

Thin-film samples are placed in the core of an inductive coil that forms part of a self-resonant ultrastable tunnel diode oscillator, with a resonant frequency around 5 MHz. The change in resonance frequency is measured as the static field is ramped from negative to positive saturation, and vice versa. This quantity is proportional to the change in inductance that in turn is governed by the transverse susceptibility ( $\chi_T$ ) of the films. The field dependence of  $\chi_T$  is plotted as a dimensionless ratio,

$$\Delta\chi_T/\chi_T(\%) = \frac{[\chi_T(H) - \chi_{\text{sat}}]}{\chi_{\text{sat}}} \times 100, \quad (1)$$

where  $\chi_{\text{sat}}$  is the transverse susceptibility at a saturation field of  $H = 5$  kOe. It should be noted that the rf field amplitude is very small (typically 1–2 Oe), and at the most can be considered only a perturbation that does not affect the magnetization in the film.

The main panel of Fig. 2(a) shows the field-dependent transverse susceptibility at room temperature, with the static magnetic field  $H$  applied perpendicular to the easy axis ( $c$  axis) for both increasing and decreasing field ramps. The striking features clearly seen in the data are the presence of identical peaks in  $\chi_T$ , symmetrically located around  $H = 0$ , with the peak positions at  $\pm 600$  Oe. This is followed by gradual approach to saturation at higher fields.

We have calculated the transverse susceptibility based on the Stoner–Wohlfarth model<sup>11,19</sup> for the same field geometry (i.e.,  $\psi = 90^\circ$ ), and this is plotted in the inset of Fig. 2(a). The remarkable qualitative agreement between the  $\chi_T$  data and the model is obvious. In particular, the fields at which singular  $\chi_T$  peaks are observed in the data can be unambiguously identified with the magnetic anisotropy fields ( $\pm H_K$ ) for this system. This is in good agreement with the values obtained from the  $M$ - $H$  loop for this geometry shown in Fig. 1(b).

The basic framework of the model can be briefly described as follows. As  $\text{CrO}_2$  is a ferromagnetic material with uniaxial anisotropy, the total-energy density can be expressed as

$$E(\theta) = K_1 \sin^2 \theta - MH \cos(\psi - \theta), \quad (2)$$

where  $K_1$  is the anisotropy constant,  $\theta$  is the angle between the magnetization vector and the easy axis, and  $\psi$  is the angle between  $H$  and the easy axis. In this expression, the magnetoelastic contribution is neglected, and only the first-order approximation to the magnetocrystalline energy is considered, as is done with standard uniaxial anisotropy.

The transverse susceptibility is then calculated by minimizing the total-energy density and determining the tensor  $dM_T/dH_T$ , where  $M_T$  and  $H_T$  are transverse components in the perpendicular direction to the applied field  $H$ . [Note that

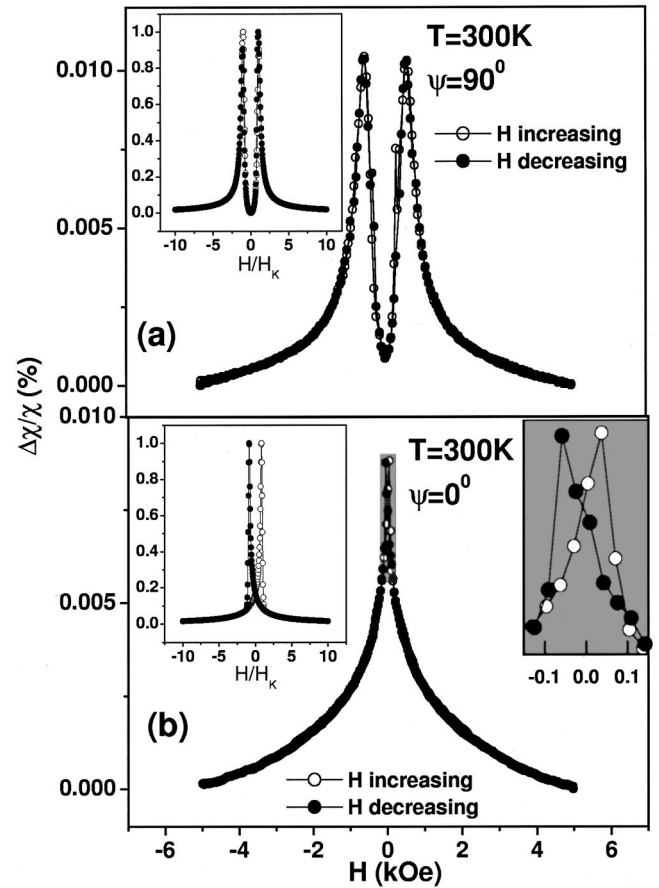


FIG. 2. (a) Measured room-temperature transverse susceptibility with static field applied perpendicular to the easy axis. Inset: Calculated  $\chi_T$  for the same geometry,  $\psi = 90^\circ$ . (b) Measured room-temperature transverse susceptibility with  $H$  applied parallel to the easy axis. Inset (right): Exploded view of the data at low fields. Inset (left): Calculated  $\chi_T$  for  $\psi = 0^\circ$ .

the rf field in the transverse direction is a very small perturbation. Thus the equilibrium position of magnetization is determined only by the static field, as expressed in Eq. (2)].

Figure 2(b) shows the experimental  $\chi_T$  for the case when  $H$  is applied parallel to the easy axis (i.e.,  $\psi = 0^\circ$ ). The inset on the right is an exploded view of the data close to  $H = 0$ , and the left inset shows the numerically calculated transverse susceptibility for this field geometry using the same model. The experimentally observed peaks in this case occur at very low fields around  $\pm 60$  Oe. While the heights of the singular peaks are suppressed (presumably due to the lack of resolution at very low fields in our measurement system), the order in which peaks occur as the field is ramped is in qualitative agreement with the theoretical model. It is important to note that unlike the case in Fig. 1(a), where two peaks are observed when the field is varied in one direction from negative to positive saturation, only one peak occurs for this geometry. This variation of the transverse susceptibility is representative of magnetization switching and the measured peak fields ( $\pm 60$  Oe) are associated with the switching fields ( $\pm H_s$ ), which are equal to the anisotropy ( $\pm H_K$ ) and coercive ( $\pm H_c$ ) fields in this case. Our results are also consistent with the  $M$ - $H$  hysteresis loops seen with  $H$  parallel to the easy axis shown in Fig. 1(a), indicating that  $\text{CrO}_2$  is a soft ferromagnetic material in this direction showing almost ideal

switching characteristics. It is also remarkable to note the large difference in  $H_K$  for  $\psi=0^\circ$  and  $90^\circ$ , which seems unique to this material and not commonly found in conventional soft ferromagnetic materials with uniaxial anisotropy. A significant property of  $\text{CrO}_2$  that clearly emerges from our experimental and theoretical  $\chi_T$  results presented in Fig. 2 is that *the sample behaves like a Stoner–Wohlfarth single-domain particle, i.e., coherent rotation dominates the magnetization process.*

Considering a low-temperature saturation magnetization of  $650 \text{ emu/cm}^3$  for the film, and taking our measured  $H_K$  value of  $600 \text{ Oe}$  from Fig. 2(a) and using the standard relation  $H_K=2K_1/M_s$ , we have estimated the anisotropy constant  $K_1$  to be  $1.9 \times 10^5 \text{ erg/cm}^3$ . This value is in agreement with  $K_1$  values reported in other studies.<sup>8,9,20</sup> However, we would like to present a note of caution that the large variation of  $H_K$  with  $\psi$  raises the issue of whether a simple picture for the magnetocrystalline anisotropy, as assumed in Eq. (2), is alone sufficient to describe the behavior in  $\text{CrO}_2$ . In fact, the higher-order anisotropy constant ( $K_2$ ) needs to be taken into account for a complete quantitative description of the magnetic anisotropy. The full angular dependence of  $H_K$ , as determined from transverse susceptibility experiments and rigorous theoretical and numerical analysis, including the higher-order terms, will be the subject of a forthcoming publication.<sup>21</sup>

The evolution of the transverse susceptibility peaks shows an interesting trend as the temperature is lowered below  $300 \text{ K}$ , and reveals yet another aspect of the magnetic anisotropy in these films. Figure 3(a) shows the field-dependent  $\chi_T$  data for four different temperatures in the geometry, where  $H$  is perpendicular to the easy axis. The normalized curves are relatively shifted by a constant value along the vertical axis for clarity. While the peaks at  $-H_K$  and  $+H_K$  remain relatively unchanged, a very sharp peak just before  $+H_K$  shows up, and rapidly increases in height at lower temperatures. In fact, this peak almost obscures the feature at  $+H_K$  to a broad shoulder at lower temperatures. Note that all the curves in Fig. 3(a) are for unidirectional field ramps from  $-5$  to  $+5 \text{ kOe}$ . For the reverse polarity, the data look identical to the peak structure positions interchanged.

Since the experimental configuration remains the same at lower temperatures as it is at  $300 \text{ K}$ , the origin of this peak must lie in the magnetic response intrinsic to the thin-film samples. We can reproduce the evolution of the peak structure using the coherent rotation model by introducing a misalignment in angle between  $H$  and the easy axis in the perpendicular geometry. This trend is clearly illustrated in Fig. 3(b), that shows a series of calculated transverse susceptibility curves for several angles deviating from the  $\psi=90^\circ$  case considered earlier.

The qualitative similarity between the measured and calculated  $\chi_T$ 's is quite striking, and suggests that as the temperature is lowered, a gradual angular misalignment develops between the applied static field and the magnetic easy axis in the sample. This effect can be accounted for by considering the influence of strain on the thin films. As noted earlier, the lattice mismatch between the  $\text{CrO}_2$  films and  $\text{TiO}_2$  substrates introduces an in-plane tensile strain. The angular misalignment as the sample temperature is lowered could be associated with changing strain. Introducing this

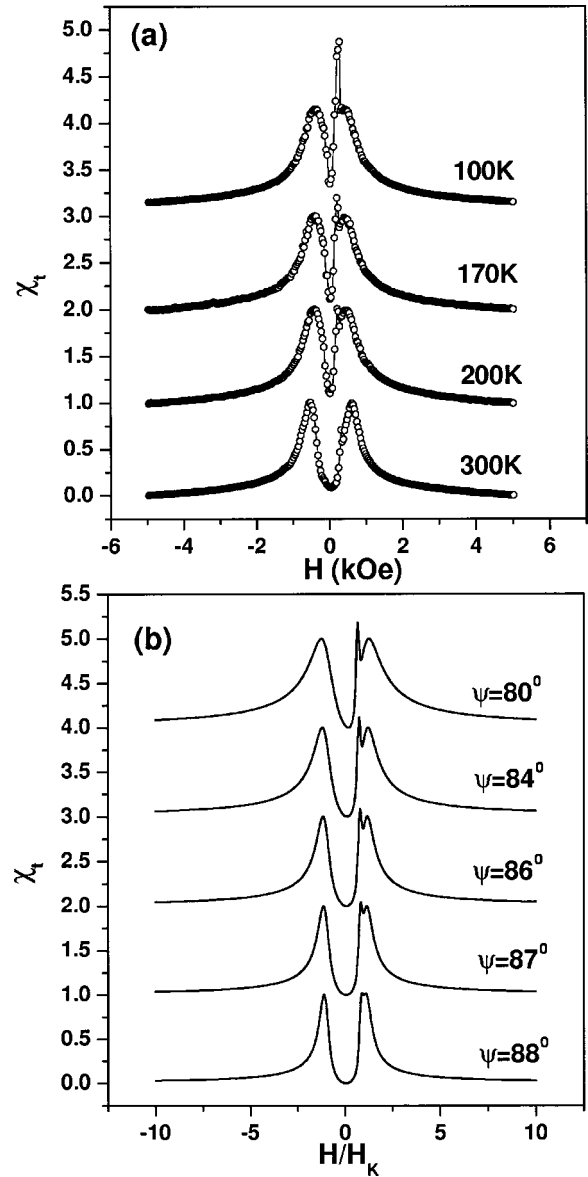


FIG. 3. (a) Measured  $\chi_T$  at different temperatures for unidirectional field ramp from  $-5$  to  $+5 \text{ kOe}$ . (b) Calculated transverse susceptibility for small angular deviations between  $H$  and the easy axis. Curves in (a) and (b) are normalized, and relatively shifted for clarity.

angular deviation between  $H$  and the easy axis is equivalent to including a net magnetoelastic energy term in the total anisotropy energy, as shown below.

The total anisotropy energy including the magnetoelastic term is

$$E_A(\theta) = \frac{M_s}{2} [H_\kappa \sin^2 \theta + H_\sigma \sin^2(\theta - \delta)], \quad (3)$$

where  $H_\sigma$  is the stress field given by

$$H_\sigma = 3\lambda_s \sigma / M_s, \quad (4)$$

where  $\lambda_s$  is the magnetostriction coefficient, and  $\sigma$  is the stress applied at an angle  $\delta$  with the easy axis. A simple transformation<sup>22</sup> of Eq. (3) can be done, yielding

$$E_A(\theta) = \frac{M_s}{2} [H^* \sin^2(\theta - \theta^*) + H^* \sin^2 \theta^* + H_\sigma \sin^2 \delta], \quad (5)$$

where

$$H^* = \sqrt{H_K^2 + H_\sigma^2 + 2H_K H_\sigma \cos 2\delta} \quad (6)$$

and

$$\tan 2\theta^* = \frac{H_\sigma \sin 2\delta}{H_K + H_\sigma \cos 2\delta}. \quad (7)$$

Therefore, the total anisotropy energy is uniaxial with the effective easy axis rotated with an angle  $\theta^*$  with respect to the magnetocrystalline easy axis.

Assuming a magnetostriction coefficient  $\lambda_s = 5 \times 10^{-6}$  from Ref. 8 and including the value of  $M_s$  and  $H_K$  from our measurements, we can estimate the stress  $\sigma$  required to cause the angular deviation of  $\theta^* = 10^\circ$  shown in Fig. 3(b) using Eqs. (4) and (7). This gives us a value of  $\sigma = 0.9 \times 10^{10}$  dyn/cm<sup>2</sup>, which is smaller than the estimated in-plane

stress values along the  $c$  and  $b$  axis due to lattice mismatch.<sup>8</sup> It has been reported that as the film thickness is reduced to  $<700 \text{ \AA}$ , the in-plane strain causes switching of the easy axis from the  $c$  direction to the  $b$  direction.<sup>8</sup> Our *transverse susceptibility results and analysis indicate that this tendency for the easy axis to gradually deviate by a small angular orientation from the  $c$  axis towards the  $b$  axis in plane is evident even for 2000-Å-thick films.* This correlation of the rf data with an increasing influence of strain at low temperatures is also consistent with the rounding of the low-temperature  $M$ - $H$  curve for  $\psi = 90^\circ$  noted in Fig. 1(b), in comparison to the room-temperature curve in Fig. 1(a). In conclusion, our experiments identify several important features in the magnetic anisotropy of epitaxially grown CrO<sub>2</sub> thin films, and this study brings forth some of the rich physics that needs further exploration in these technologically important oxides.

The work at AMRI is supported through DARPA Grant No. MDA 972-97-1-003. G.X. acknowledges support from the NSF through Grant No. DMR-0071770.

- 
- <sup>1</sup>G. Prinz, Phys. Today **48** (4), 58 (1995).  
<sup>2</sup>D. D. Awschalom and J. M. Kikkawa, Phys. Today **52** (6), 33 (1999).  
<sup>3</sup>A. Gupta and J. Z. Sun, J. Magn. Magn. Mater. **200**, 24 (1999).  
<sup>4</sup>K. P. Kamper, W. Schmitt, G. R. J. Gambino, and R. Ruf, Phys. Rev. Lett. **59**, 2788 (1987).  
<sup>5</sup>R. J. Soulen, Jr., J. M. Byers, M. S. Osofsky, B. Nadgorny, T. Ambrose, S. F. Cheng, P. R. Broussard, C. T. Tanaka, J. Nowak, J. S. Moodera, A. Barry, and J. M. D. Coey, Science **282**, 85 (1998).  
<sup>6</sup>J. M. D. Coey, A. E. Berkowitz, Ll. Balcells, and F. F. Putris, Phys. Rev. Lett. **80**, 3815 (1998).  
<sup>7</sup>H. Y. Hwang and S. W. Cheong, Science **278**, 1607 (1997).  
<sup>8</sup>X. W. Li, A. Gupta, and G. Xiao, Appl. Phys. Lett. **75**, 713 (1999).  
<sup>9</sup>F. Y. Yang, C. L. Chien, E. F. Ferrari, X. W. Li, Gang Xiao, and A. Gupta, Appl. Phys. Lett. **77**, 286 (2000).  
<sup>10</sup>S. Sundar Manoharan, D. Elefant, G. Reiss, and J. B. Goodenough, Appl. Phys. Lett. **72**, 984 (1998).  
<sup>11</sup>E. C. Stoner and E. P. Wohlfarth, Proc. R. Soc. London, Ser. A **240**, 599 (1948).  
<sup>12</sup>X. W. Li, A. Gupta, T. R. McGuire, P. R. Duncombe, and G. Xiao, J. Appl. Phys. **85**, 5585 (1999).  
<sup>13</sup>L. Paretti and G. Turilli, J. Appl. Phys. **61**, 5098 (1987).  
<sup>14</sup>A. Hoare, R. W. Chantrell, W. Schmitt, and A. Eiling, J. Phys. D **26**, 461 (1993).  
<sup>15</sup>R. W. Chantrell, A. Hoare, D. Melville, H. J. Lutke-Stetzkamp, and S. Methfessel, IEEE Trans. Magn. **25**, 4216 (1989).  
<sup>16</sup>M. Prutton, J. Appl. Phys. **39**, 1153 (1968).  
<sup>17</sup>H. Srikanth, J. Wiggins, and H. Rees, Rev. Sci. Instrum. **70**, 3097 (1999).  
<sup>18</sup>L. Spinu, H. Srikanth, E. E. Carpenter, and C. J. O'Connor, J. Appl. Phys. **87**, 5490 (2000).  
<sup>19</sup>A. Aharoni, E. H. Frei, S. Shtrikman, and D. Treves, Bull. Res. Council Isr., Sect. F **6A**, 215 (1957).  
<sup>20</sup>D. S. Rodbell, J. Phys. Soc. Jpn. **21**, 1224 (1966).  
<sup>21</sup>L. Spinu *et al.* (unpublished).  
<sup>22</sup>O. Caltun, L. Spinu, and A. Stancu, Sens. Actuators **59**, 142 (1997).